International Journal of Theoretical Physics, Vol. 42, No. 11, November 2003 (© 2003)

Quantum Mechanics of Two-Field Parametric Frequency Converter Interacting with a Single Atom

M. Sebawe Abdalla,[1] A. S.-F. Obada,[2,3] and E. M. Khalil[2]

Received April 17, 2003

In this communication we deal with a new model Hamiltonian representing the interaction between a two-level atom and two electromagnetic field modes in a cavity. The interaction between the modes has been taken into account and considered to be of a parametric frequency converter type. The model can be regarded as a generalization of two different systems: the Jaynes–Cummings model (atom–field interaction) and the two-mode frequency converter model (field–field interaction). Under a certain condition an exact solution for the equations of motion in the Heisenberg picture is given. The wavefunction in the Schrödinger picture is also constructed and used to discuss some statistical properties related to the model. We assume that the fields are initially in coherent states. We discuss atomic inversion, photon number distribution, squeezing and other phenomena. We show in all cases that the system is very sensitive to any variation in the mean photon numbers.

KEY WORDS: parametric frequency converter; Jaynes–Cummings model; squeezing; Q-function.

1. INTRODUCTION

It is well known that the interaction of a single two-level atom with the quantized electromagnetic field of a lossless high-Q cavity is a central problem in cavity quantum electrodynamics (Filipowicz *et al.*, 1985, 1986; Guzman *et al.*, 1989, Meschede *et al.*, 1985; Rempe *et al.*, 1987). The simplest physical situation may be described by the well known and today fundamental Jaynes–Cummings model (JCM) (Jaynes and Cummings, 1963). Despite being simple enough to be analytically soluble in the rotating wave approximation (RWA), this model has been a source of insight into the nuances of the interaction between light and matter. It has allowed a deeper understanding of the dynamical entangling

[1] Mathematics Department, College of Science, King Saud University, Riyadh, Saudi Arabia.
[2] Department of Mathematics, Faculty of Science, Al-Azher University, Nasr City, Cairo, Egypt.
[3] To whom correspondence should be addressed at Department of Mathematics, Faculty of Science, Al-Azher University, Nasr City 11884, Cairo, Egypt; e-mail: obada75@hotmail.com.

0020-7748/03/1100-2735/0 © 2003 Plenum Publishing Corporation

and disentangling of the atom-field system over the course of time. It has also led to nontrivial predictions, such as the collapse–revival phenomenon (Eberly *et al.*, 1980; Narozhny *et al.*, 1981), vacuum-field Rabi splitting, sub-Poissonian statistics, antibunching (Diedrich and Walther, 1987; Short and Mandel, 1983), squeezing (Kuklinski and Madajczyk, 1988; Short and Mandel, 1983), chaos, and trapping states (Gea-Bancloche, 1990, 1991; Milonni *et al.*, 1983a,b; Phoenix and Knight, 1988, 1991a,b; Slosser *et al.*, 1989; Slosser and Meystre, 1990). In fact the complex dynamical evolution and the fully quantum nature of the model have turned it into a laboratory for theorists and the basis of many more elaborate models.

The Hamiltonian model describing such a system is given by

$$\frac{\hat{H}}{\hbar} = \omega \hat{a}^\dagger \hat{a} + \frac{\omega_0}{2}\hat{\sigma} + \lambda(\hat{a}^\dagger \hat{\sigma}_- + \hat{a}\hat{\sigma}_+), \tag{1}$$

where ω is the field frequency, $\hat{a}^\dagger$ and $\hat{a}$ are the field creation and annihilation operators satisfying the commutation relation $[\hat{a}, \hat{a}^\dagger] = 1$, while λ is the coupling constant, and ω_0 is the natural transition frequency of the atom, $\sigma_\pm$, and σ_z are the usual 2×2 Pauli matrices satisfying

$$[\sigma_z, \sigma_\pm] = \pm 2\sigma_\pm, \quad [\sigma_+, \sigma_-] = \sigma_z. \tag{2}$$

There are a huge number of papers considering this model in great detail. Most of these papers concentrate on the statistical behavior as well as the dynamics of the model; for more details see Shore and Knight (1993) and the references therein. However, to meet the experimental realization, there are several attempts to generalize and modify this model into different directions. For instance it has been generalized and extended to include the effects of cavity mode decay as well as black-body photons (Knight and Radmore, 1982; Puri and Joshi, 1989). Furthermore we can see the consideration of multimode and multiphoton instead of single mode and single photon processes (Abdalla *et al.*, 1990, 1991, 2002), addition of Kerr-like medium (Buzek and Jex, 1990; Joshi and Puri, 1992; Werner and Risken, 1991a,b), and Stark shift, among other modifications (Abdel-Aty *et al.*, 2002; Gou *et al.*, 1997; Moya *et al.*, 1991). We may also refer to Tavis–Cummings model (TCM) as a generalization of JCM (Deng, 19983; Joshi and Lawande, 1991; Tavis *et al.*, 1966) where the angular momentum operators replace the Pauli matrices to study multilevel atom instead of two-level atom (Bogolubov *et al.*, 1984; Makhviladze and Shelepin, 1974). In the meantime it has been observed that if the interaction occurs between more than one field, mode none of the above workers considered modifications to include the interaction between the field modes themselves. In the present communication, we shall fill this gap and introduce a new Hamiltonian model taking the interaction between the fields to be of a parametric frequency type (Glauber, 1963). In fact parametric frequency conversion occurs in a number of well-known phenomena including the production of anti-Stokes

radiation in Brillouin and Raman scattering, and the upconversion of light signals in nonlinear media. Furthermore parametric up conversion is of interest for the conversion of infrared wavelengths into the visible part of the spectrum where fast and efficient detection is possible using photomultipliers (Abdalla *et al.*, 2001a,b; El-Orany *et al.*, 2001a,b,c).

The model we shall introduce consists of two modes of the cavity field interacting with a single atom within a perfect cavity. The interaction between the fields will be taken into account where we assume it to be of parametric frequency converter type. In this case the model we shall consider takes the form

$$\frac{\hat{H}}{\hbar} = \sum_{i=1}^{2}[\omega_i \hat{a}_i^\dagger \hat{a}_i + \lambda_i(\hat{a}_i^\dagger \hat{\sigma}_- + \hat{a}_i \hat{\sigma}_+)] + \frac{\omega_0}{2}\hat{\sigma}_z + \lambda_3(\hat{a}_1^\dagger \hat{a}_2 + \hat{a}_1 \hat{a}_2^\dagger), \qquad (3)$$

where ω_i, $i = 1, 2$ are the fields frequencies, and ω_0 has the same meaning as in Eq. (1), while λ_i, $i = 1, 2$ are the coupling constants between the modes and the atom. The last term of the above Hamiltonian represents the interaction between the modes where λ_3 is the coupling parameter. The operators $\hat{a}_i$ and $\hat{a}_j^\dagger$ are the usual Boson operators for the quantized fields mode which obey $[\hat{a}_i, \hat{a}_j] = \delta_{ij}$, where $\delta_{ij} = 1$ if $i = j$, and zero otherwise.

The Hamiltonian (3) can be regarded in one side as a generalization of the Jaynes–Cummings model and in the other side as a two field parametric frequency model. This is quite obvious from the comparison between Eqs. (1) and (3) where the effect of the second mode as well as the interaction between the fields are apparent from the existence of the coupling parameters λ_2 and λ_3, respectively. The main purpose of the present paper is to consider the atomic inversion as well as to discuss some statistical properties related to the Hamiltonian of Eq. (3). To reach our goal we have to find the exact time-dependent expressions for the dynamical operators $\hat{a}_i$ and $\sigma's$. This can be achieved by solving the equations of motion in the Heisenberg picture.

For this purpose we devote section 2 to giving the exact solution for the equations of motion. In section 3 we shall consider the probability amplitude as well the atomic inversion, while in section 4 we discuss the correlation function followed by a discussion related to the squeezing phenomenon in section 5. We have also devote section 6 to consider the second-order correlation function for each mode. While in section 7 we discuss the behavior of the Q-function, followed by a consideration of the phase distribution and quantum field entropy in 7 and 10, respectively.

2. DYNAMICAL OPERATORS AND THE WAVEFUNCTION

Our aim in this section is to concentrate on finding the dynamical operators expression for both atomic and fields for the present system. Also we shall introduce

the exact formula for the wavefunction in Schrödinger represtation. Both of these expressions will be used later in our discussion for the statistical properties of the model. For this reason let us first find the solution of the Heisenberg equations of motion. To do so we introduce the canonical transformation

$$\hat{a}_1 = \hat{b}_1 \cos\xi + \hat{b}_2 \sin\xi, \quad \hat{a}_2 = \hat{b}_2 \cos\xi - \hat{b}_1 \sin\xi, \tag{4}$$

where $\xi = \frac{1}{2}\tan^{-1}(\frac{2\lambda_3}{\omega_2-\omega_1})$, and the operators $\hat{b}_i$ and $\hat{b}_j^\dagger$ satisfy the commutation relation $[\hat{b}_i, \hat{b}_j] = \delta_{ij} = 1$ if $i = j$ and *zero* otherwise. In this case the Hamiltonian (3) takes the form

$$\frac{\hat{H}}{\hbar} = \sum_{i=1}^{2} \Omega_i \hat{b}_i^\dagger \hat{b}_i + \frac{\omega_0}{2}\sigma_z + \delta_1(\hat{b}_1^\dagger\sigma_- + \hat{b}_1\sigma_+) + \delta_2(\hat{b}_2^\dagger\sigma_- + \hat{b}_2\sigma_+) \tag{5}$$

where δ_i, $i = 1, 2$ are the modified coupling parameters given by

$$\delta_1 = (\lambda_1 \cos\xi - \lambda_2 \sin\xi), \text{ and } \delta_2 = (\lambda_2 \cos\xi + \lambda_1 \sin\xi), \tag{6}$$

and Ω_i, $i = 1, 2$ are the new free frequencies of fields such that

$$\begin{aligned}\Omega_1 &= (\omega_1 \cos^2\xi + \omega_2 \sin^2\xi - \lambda_3 \sin 2\xi), \text{ and}\\ \Omega_2 &= (\omega_2 \cos^2\xi + \omega_1 \sin^2\xi + \lambda_3 \sin 2\xi).\end{aligned} \tag{7}$$

Before we go further let us assume the states $|m_1, m_2\rangle_a$ (say) corresponding to the physical operators $\hat{a}_i$ and $\hat{a}_i^\dagger$, $i = 1, 2$ such that $\hat{a}_1|m_1, m_2\rangle = \sqrt{m_1}|m_1 - 1, m_2\rangle$ and $\hat{a}_2|m_1, m_2\rangle = \sqrt{m_2}|m_1, m_2 - 1\rangle$ and the states $|n_1, n_2\rangle_b$ corresponding to the rotated operators $\hat{b}_j$ and $\hat{b}_j^\dagger j = 1, 2$ with properties similar to that of the operators $\hat{a}_i$ and $\hat{a}_i^\dagger$. Then the connection between the two states are given by

$$\begin{aligned}|m_1, m_2\rangle_a = \sum_{i=0}^{m_1}\sum_{i=0}^{m_2}(-)^j \binom{m_1}{i}\binom{m_2}{j}\left(\frac{n_1!n_2!}{m_1!m_2!}\right)^{\frac{1}{2}}\\ \times (\cos\xi)^{m_2-j+i}(\sin\xi)^{m_1-i+j}|n_1, n_2\rangle_b,\end{aligned} \tag{8}$$

where $n_1 = i + j$, and $n_2 = m_1 + m_2 - i - j$. In this case one can show that $\hat{a}_i^\dagger\hat{a}_i|m_1, m_2\rangle_a = m_i|m_1, m_2\rangle_a$, $i = 1, 2$ and similarly for the other operators $\hat{b}_j^\dagger\hat{b}_j^\dagger|n_1, n_2\rangle_b = n_j|n_1, n_2\rangle_b$, $j = 1, 2$. Furthermore if we assume that α_i, $i = 1, 2$ is the eigenvalues of the oparators $\hat{a}_i$ with respect the coherent state $|\alpha_i\rangle$ and β_j, $j = 1, 2$ are the eigenvalues of the oparators $\hat{b}_j$ with respect to the coherent states $|\beta_j\rangle$. Then the relation between the two eigenvalues is

$$\alpha_1 = \beta_1 \cos\xi + \beta_2 \sin\xi, \quad \alpha_2 - \beta_2 \cos\xi - \beta_1 \sin\xi,$$

It is well known that for any operator $\hat{O}$ the Heisenberg equation of motion is given by

$$\frac{d\hat{O}}{dt} = \frac{\partial \hat{O}}{\partial t} + \frac{1}{i\hbar}[\hat{O}, \hat{H}], \tag{9}$$

therefore the equations of the motion for the Hamiltonian (5) are

$$\begin{aligned}
&\frac{d\hat{b}_1}{dt} = -i\Omega_1\hat{b}_1 - i\delta_1\hat{\sigma}_-, \quad \frac{d\hat{b}_2}{dt} = -i\Omega_2\hat{b}_2 - i\delta_2\sigma_-,\\
&\frac{d\hat{\sigma}_-}{dt} = -i\omega_0\hat{\sigma}_- + i(\delta_1\hat{b}_1 + \delta_2\hat{b}_2)\hat{\sigma}_z,\\
&\frac{d\hat{\sigma}_z}{dt} = 2i\delta_1(\hat{b}_1^\dagger\hat{\sigma}_- - \hat{b}_1\hat{\sigma}_+) + 2i\delta_2(\hat{b}_2^\dagger\hat{\sigma}_- - \hat{b}_2\hat{\sigma}_+).
\end{aligned} \tag{10}$$

However because of the difficulty of solving the system of equations resulting from the Heisenberg equations of motion we shall adjust the coupling parameter λ_3 to take the form

$$\lambda_3 = \frac{\lambda_1\lambda_2}{(\lambda_1 + \lambda_2)}\varepsilon, \text{ where } \varepsilon = \frac{\omega_2 - \omega_1}{\lambda_2 - \lambda_1} \tag{11}$$

In this case the restrictive condition (11) implies that the coupling parameter δ_1 tends to zero while δ_2 survives and equals to $\eta = \sqrt{\lambda_1^2 + \lambda_2^2}$. After straightforward calculations the general solution of Eqs. (10) are given by

$$\begin{aligned}
\hat{b}_1(t) &= \hat{b}_1(0)\ \exp(-i\Omega_1 t),\\
\hat{b}_2(t)^{i\omega t} &= e^{i\hat{C}t}\left[\left[\cos(\gamma t) - i\frac{\hat{C}}{\gamma}\ \sin(\gamma t)\right]\hat{b}_2(0) - i\frac{\eta}{\gamma}\ \sin(\gamma t)\hat{\sigma}_-(0)\right],\\
\hat{\sigma}_-(t)^{i\omega t} &= e^{i\hat{C}t}\left[\left[\cos(\gamma t) + i\frac{\hat{C}}{\gamma}\ \sin(\gamma t)\right]\hat{\sigma}_-(0) - i\frac{\eta}{\gamma}\ \sin(\gamma t)\hat{b}_2(0)\right],\\
\hat{\sigma}_z(t) &= \left(\cos(2\hat{C}t) - i\frac{\Delta}{2C}\ \sin(2\hat{C}t)\right)\hat{\sigma}_z(0) + \frac{\sin(2\hat{C}t)}{C}[\hat{C}\\
&\quad - 2\eta\hat{b}_2(0)\hat{\sigma}_+(0)] + \frac{\sin^2(\hat{C}t)}{C},
\end{aligned} \tag{12}$$

where

$$\hat{C} = \frac{\Delta}{2}\hat{\sigma}_z + \eta(\hat{b}_2\hat{\sigma}_+ + \hat{b}_2^\dagger\hat{\sigma}_-), \tag{13}$$

and $\Delta = (\omega_0 - \Omega_2)$ represents the detuning parameter. The quantity γ and C in

Eq. (12) are

$$\gamma = \left[\frac{\Delta^2}{4} + \eta^2(\hat{b}_2^\dagger \hat{b}_2 \hat{\sigma}_+ + \hat{\sigma}_- + 1)\right]^{\frac{1}{2}}, \text{ and } C = \left[\frac{\Delta^2}{4} + \eta^2(\hat{b}_2^\dagger \hat{b}_2 + \hat{\sigma}_+ \hat{\sigma}_-)\right]^{\frac{1}{2}}, \tag{14}$$

Having obtained the dynamical operators expressions for the Hamiltonian model (5), we are therefore in position to discuss the statistical properties of the present system. However, it will be also convenient to construct the wavefunction in Schrödinger picture. Thus if we consider that, at time $t = 0$, the atom is prepared in its coherent excited state $|\theta, \phi\rangle = [\cos\frac{\theta}{2}|e\rangle + \sin\frac{\theta}{2}e^{-i\phi}|g\rangle]$, and both fields are considered to be initially in a coherent states, then the initial wavefunction of the system can be written as

$$|\psi(0)\rangle = \sum_{n_1,n_2=0}^{\infty}\left[q_{n_1,n_2}\left[\cos\frac{\theta}{2}|e\rangle + \sin\frac{\theta}{2}e^{-i\phi}|g\rangle\right]\otimes|n_1, n_2\rangle_b\right]. \tag{15}$$

After some algebric manipulations the wavefunction at $t \succ 0$ will take the form

$$\begin{aligned}|\psi(t)\rangle = &\sum_{n_1,n_2=0}^{\infty}\Bigg[\cos\frac{\theta}{2}\{F_1(n_2,t)\}q_{n_1,n_2}\\ &- ie^{-i\phi}\sin\frac{\theta}{2}e_1(n_2,t)\{\nu_1(n_2)q_{n_1,n_2+1}\}\Bigg]|n_1,n_2\rangle_b\otimes|e\rangle\\ &+\sum_{n_1,n_2=0}^{\infty}\Bigg[e^{-i\phi}\sin\frac{\theta}{2}\bar{F}_2(n_2,t)q_{n_1,n_2}\\ &- i\cos\frac{\theta}{2}e_2(n_2,t)\nu_2(n_2,t)q_{n_1,n_2-1}\Bigg]|n_1,n_2\rangle_b\otimes|g\rangle.\\ = &\sum_{n_1,n_2=0}^{\infty}[A(n_1,n_2,t)|n_1,n_2\rangle_b\otimes|e\rangle + B(n_1,n_2,t)|n_1,n_2\rangle_b\otimes|g\rangle],\end{aligned} \tag{16}$$

where

$$\begin{aligned}F_j(n_2,t) &= \left(\cos\hat{\mu}_j(n_2)t - \frac{i\Delta}{2\mu_j(n_2)}\sin\hat{\mu}_j(n_2)t\right),\\ e_j(n_2,t) &= \frac{\sin\hat{\mu}_j(n_2)t}{\mu_j(n_2)t}, \quad \mu_j^2(n_2) = \left[\frac{\Delta^2}{4} + \nu_j(n_2)\right], \quad j = 1,2\end{aligned} \tag{17}$$

with

$$\nu_1(n_2) = \eta^2(n_2+1), \quad \hat{\nu}_2(n_2) = \eta^2 n_2, \tag{18}$$

and the function $\bar{F}_i$, $i = 1, 2$ in Eq. (16) is the complex conjugate of the function F_i.

Now let us introduce a combination between the operators $\hat{b}_1$ and $\hat{b}_2$ which will be more convenient for us to use. This may be written as

$$\begin{aligned} H(l, m, r, p, t) &= \langle\psi(t)|\hat{b}_1^{\dagger l}\hat{b}_1^m\hat{b}_2^{\dagger r}\hat{b}_2^p|\psi(t)\rangle \\ &= \exp(-|\beta_2|^2)\beta_1^m\beta_1^{*l}\beta_2^p\beta_2^{*r}\sum_{n_2=0}^{\infty}\frac{|\beta_2|^{2n_2}}{n_2!}\big[F_1(n_2+p,t) \\ &\quad\times\bar{F}_1(n_2+r,t) \\ &\quad+|\beta_2|^{-2}\sqrt{(n_2+p)(n_2+r)}e_2(n_2+p,t)\times e_2(n_2+r,t) \\ &\quad\sqrt{\nu_2(n_2+p)\nu_2(n_2+r)}\big], \end{aligned} \tag{19}$$

The above formula will be usefull for us, and we shall use it later. Further let us introduce the reduced density operator $\rho^f(t)$ as follows

$$\rho^f(t) = |A(t)\rangle\langle A(t)| + |B(t)\rangle\langle B(t)|, \tag{20}$$

where $|A(t)\rangle$ and $|B(t)\rangle$ are defined through Eq. (16). In the forthcoming sections we shall employ the results obtained here to discuss some statistical properties for the present model.

3. ATOMIC INVERSION

Atomic population inversion can be considered as the simplest important quantity in the JCM. It is defined as the difference between the probabilities of finding the atom in the exited state and in the ground state. When the atom is in the excited state, the atomic inversion is given by

$$W(t) = \frac{1}{2}e^{-|\beta_2|^2}\sum_{n_2=0}^{\infty}\frac{\overline{n_2}^{n_2}}{n_2!}\{|F_1(n_2,t)|^2 - [e_1(n_2,t)\nu_1(n_2)]^2\}, \tag{21}$$

whence we find the phenomenon of collapses and revivals similar to that of the coherent state JCM case. Since the revival times can be estimated (Eberly *et al.*, 1980; Gerry and Hach, 1993; Moya-Cessa and Vidiella-Barranco, 1995; Narozhny *et al.*, 1981; Vidiella-Barranco *et al.*, 1992), the revival times for a coherent state can be written as $t_R = 2\pi\sqrt{n_2}$. In our numerical investigations we plot the atomic inversion against time t taking into consideration the atom initially in the excited state and the field is prepared for different cases. In all cases we consider here it should be noted that we assum the parameters $\theta = \phi = 0$. In Fig. 1(a) we have taken the two fields parameter $\alpha_1 = -\alpha_2 = 3$, and the coupling parameters ratio $\lambda_1/\lambda_2 = 1.1$ which represents very weak field (almost vacuum). In this case we see in absence of the detuning parameter (resonance case $\Delta = 0$) that there are regular

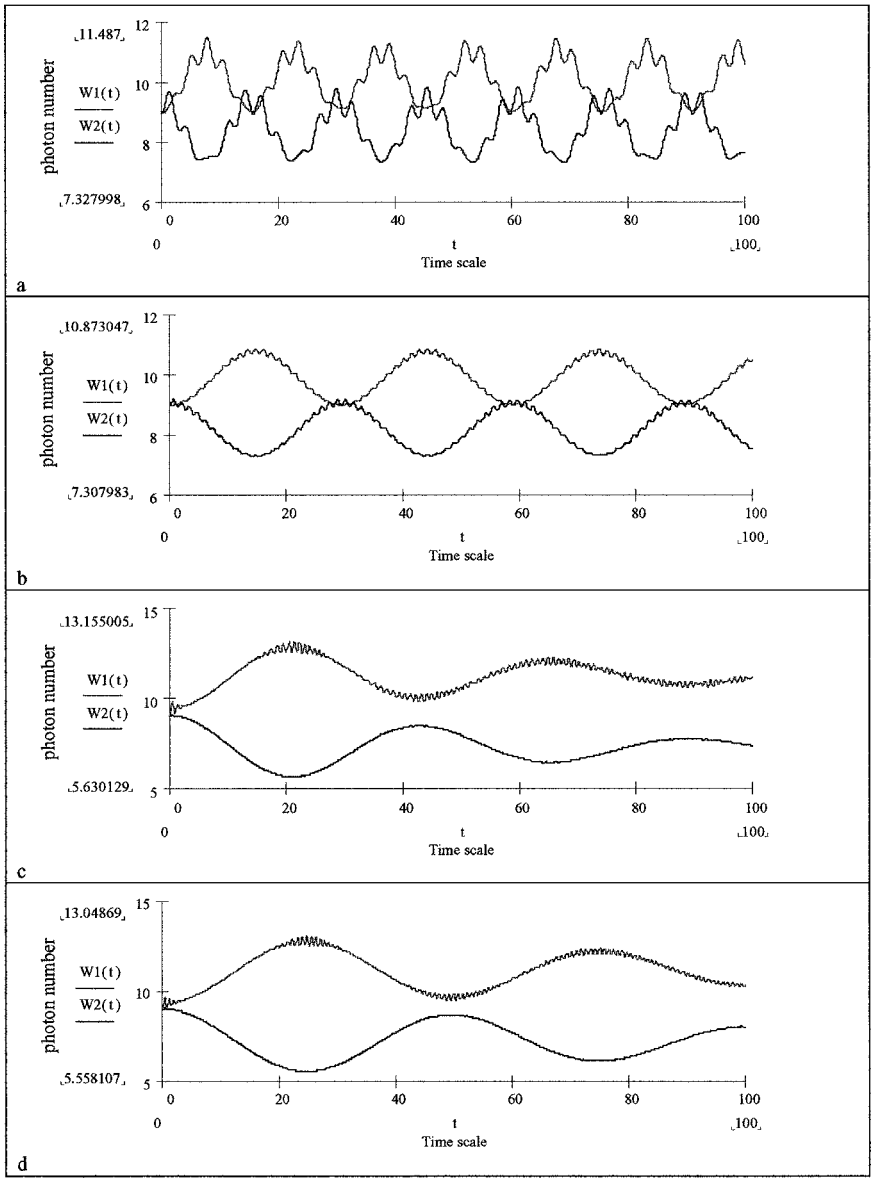

Fig. 1. The evolution of the atomic inversion against time t the atom initially in excited state ($\theta = 0$ and $\phi = 0$) and the field is prepared in some different cases. (a) $\alpha_1 = -\alpha_2 = 3$, $\lambda_1/\lambda_2 = 1.1$ and $\Delta = 0$; (b) $\Delta = 4$ and other parameters same as (a); (c) $\alpha_1 = \alpha_2 = 3$, $\lambda_1/\lambda_2 = 0.1$; and $\Delta = 0$; (d) $\Delta = 4$ and other parameters same as (c); (e) $\alpha_1 = \alpha_2 = 3$, $\lambda_1/\lambda_2 = 1.1$ and $\Delta = 0$, (f) $\Delta = 4$ and other parameters same as (e).

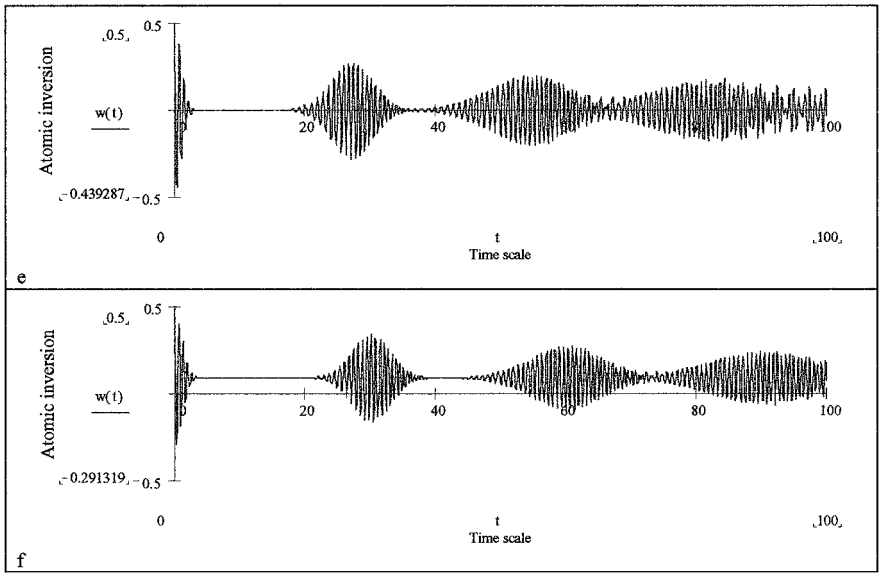

Fig. 1. (*Continued.*)

oscillations around $W(t) = 0$ where no collapses and revivals can be observed. Similar observation can be seen for the off-resonance case when $\Delta = 4$, where we can see regular oscillations around $W(t) = 0.4$ but without any observation of the collapses and revivals phenomenon, however there is a rapid fluctuations occurred in the function, see Fig. 1(b). On contrary when the two fields parameter take the values $\alpha_1 = \alpha_2 = 3$, and the coupling parameters ratio $\lambda_1/\lambda_2 = 0.1$, corresponding to slightly weak field ($\bar{n}_2 \sim 9$), the situation is drastically changed. In this case and in absence of the detuning parameter (exact resonance case), we can realize for $t_R = 2\pi\sqrt{n_b}$ that after short period of collapse the function shows long revival period followed by another collapses period, however as the time goes on we can see very weak revivals appeared at different period of the time during the course of the interaction, see Figs. 1(c). When the detuning parameter takes place $\Delta = 4$ we can see an increase in the revivals period and both collapses and revivals are apparent, however the function value is shifted upwards, see Fig. 1(d). Same conclusion may be given for the case in which the coupling parameters ratio $\lambda_1/\lambda_2 = 1.1(\bar{n}_2 \sim 18)$ with the same value of the field parameters $\alpha_1 = -\alpha_2 = 3$. In this case the exact resonance shows fluctuations around zero, while for the nonresonance case the mean value of the atomic inversion is shifted upwards which means that the energy is inherent in the atomic system, see Fig. 1(e) and (f).

4. PHOTON NUMBER DISTRIBUTION

In this section we shall discuss the behavior of the photon numbers related to the present system. When the atom starts from its excited state we can write the mean number of photons for each mode which is related to the physical modes according to the following formulae

$$\langle \bar{n}_1(t)\rangle = H(1,1,0,0)\cos^2\xi + Re(H(1,0,0,1))\sin 2\xi + H(0,0,1,1)\sin^2\xi, \tag{22}$$

and

$$\langle \bar{n}_2(t)\rangle = H(1,1,0,0)\sin^2\xi - Re(H(1,0,0,1))\sin 2\xi + H(0,0,1,1)\cos^2\xi. \tag{23}$$

In the present case the Rabi frequency is proportional to $\sqrt{(n_2+1)}$, which is similarly to that of the single mode JCM case. This is in fact due to the canonical transformation and the restricted condition which have been used to transform the present system to a single mode case. We have plotted in Fig. 2 the expectation value of the photon numbers $\langle \bar{n}_1(t)\rangle$ and $\langle \bar{n}_2(t)\rangle$ against the time t for different values of the parameters α_1, α_2, λ_1, λ_2, and the detuning parameter Δ. For example when we take the parameters $\alpha_1 = -\alpha_2 = 3$, and the ratio of the coupling parameters $\lambda_1/\lambda_2 = 1.1$ with fixed value of the parameters $\theta = 0$, and $\phi = 0$, we can observe in the resonance case $\Delta = 0$ that, there are slow and irregular oscillations with slight intersection between the two functions. This is quite obvious from an oscillating envelope appearing in Fig. 2(a). However when the detuning parameter is taken into consideration $\Delta = 4$ (off-resonance case), we find there are rapid oscillations, however with small amplitude imposed on slowly oscillating envelope as shown in Fig. 2(b). In addition we can also see in this case more regularity in the functions behavior which is on the contrary to the exact resonance case. For the case in which the parameters $\alpha_1 = \alpha_2 = 3$, we have plotted Figs. 2(c)–(f) for the same values of the other parameters. We have observed that in both cases resonance and off-resonance there are rapid oscillations with small amplitude imposed on an oscillating envolope. Also we can mention that there no intersection occurs between the two function during the whole period of the time considered. This difference is due to the appearance of the middle terms in both Eqs. (22) and (23) which is the source of the oscillating envelope as can be seen clearly from the figures. This means that the first mode gains energy at the expense of the second mode.

5. SQUEEZING PHENOMENON

Investigation of the squeezing properties of the radiation field is a central topic in quantum optics. For this reason we devote this section to discuss the squeezing

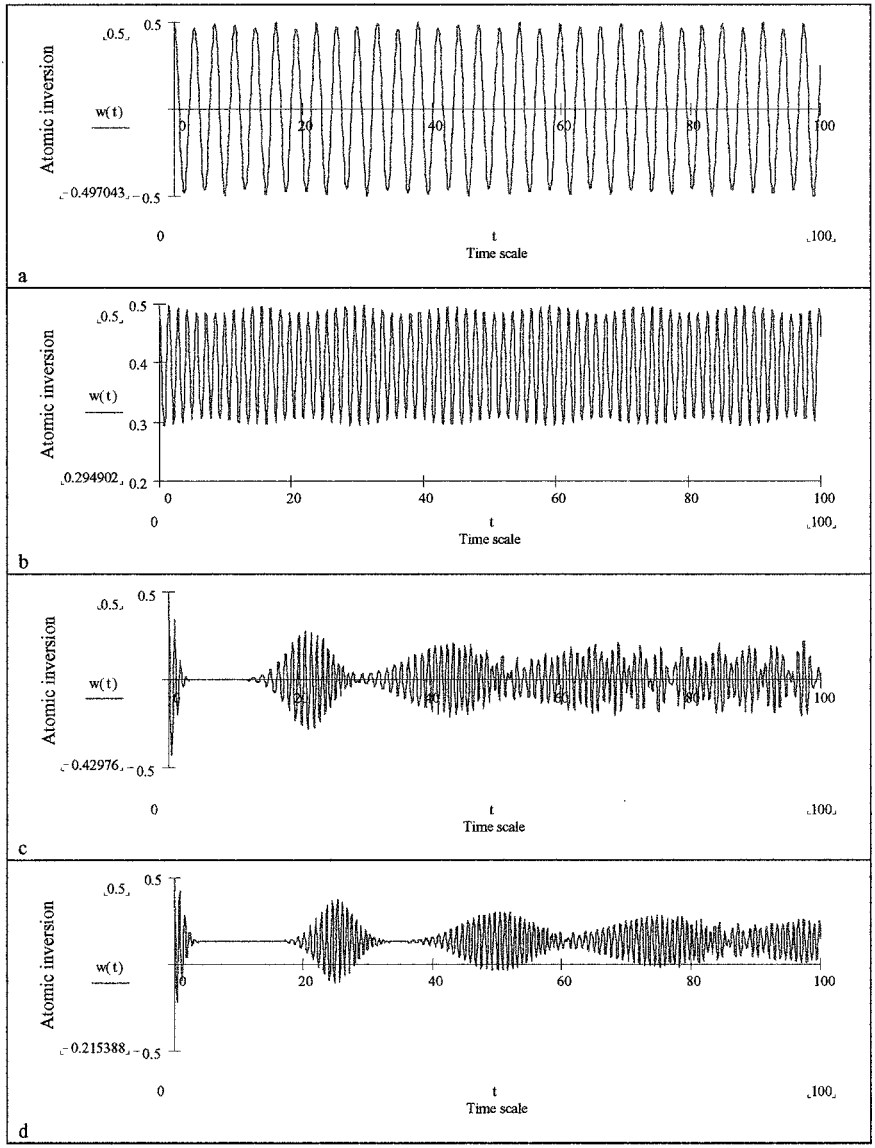

Fig. 2. The evolution of the photon number operator against time t the atom initially in excited state ($\theta = 0$ and $\phi = 0$) and the field is prepared in some different cases. (a) $\alpha_1 = -\alpha_2 = 3$, $\lambda_1/\lambda_2 = 1.1$ and $\Delta = 0$; (b) $\Delta = 4$ and other parameters same as (a); (c) $\alpha_1 = \alpha_2 = 3$, $\lambda_1/\lambda_2 = 0.1$ and $\Delta = 0$, (d) $\Delta = 4$ and other parameters same as (c); (e) $\alpha_1 = \alpha_2 = 3$, $\lambda_1/\lambda_2 = 1.1$ and $\Delta = 0$; (f) $\Delta = 4$ and other parameters same as (e).

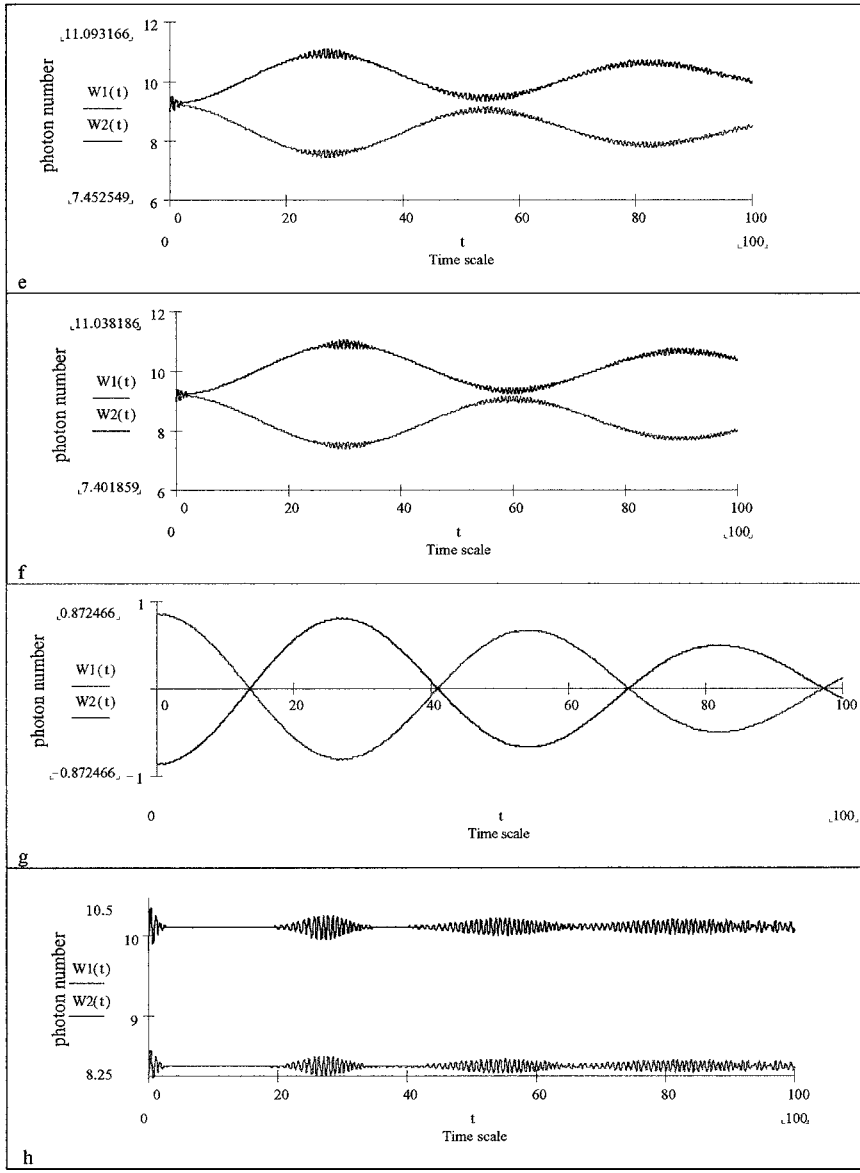

Fig. 2. (*Continued.*)

phenomenon related to the present system. In fact, squeezed light is a radiation field without a classical analogue, one of whose quadratures of the electric field has less fluctuations than those for a coherent state at the expense of increased fluctuations in the other quadrature, such that the Heisenberg uncertainty relation is fulfilled. The usefulness of such light relates to several applications in optical communication networks (Shapiro *et al.*, 1979; Yuen and Shapiro, 1978, 1980), to interferometric techniques (Caves and Schumaker, 1985; Schumaker and Caves, 1985), and to optical waveguide tap (Shapiro, 1980). Generation of squeezed light has been observed in many optical processes (Loundon and Knight, 1987; Meystre and Walls, 1991). We shall here concentrate on discussing the two mode normal squeezing, and therefore to reach our goal we must calculate the variances of the two slowly varying quadratures of

$$\hat{x} = \frac{1}{2\sqrt{2}}(\hat{a}_1^\dagger + \hat{a}_1 + \hat{a}_2^\dagger + \hat{a}_2) \text{ and } \hat{y} = \frac{i}{2\sqrt{2}}(\hat{a}_1^\dagger - \hat{a}_1 + \hat{a}_2^\dagger - \hat{a}_2) \tag{24}$$

These operators satisfy the commutation relation $[\hat{x}, \hat{y}] = \frac{i}{2}$ and the uncertainty relation

$$(\Delta\hat{x})^2(\Delta\hat{y})^2 \geq \frac{1}{16}. \tag{25}$$

The state of the field is said to be squeezed whenever one of the two quadratures $\hat{x}$ and $\hat{y}$ satisfies the relation

$$\langle(\Delta\hat{x})^2\rangle \text{ or } \langle(\Delta\hat{y})^2\rangle \prec \frac{1}{4}. \tag{26}$$

The variance $\langle(\Delta\hat{x})^2\rangle = \langle\hat{x}^2\rangle - \langle\hat{x}^2\rangle$ is given in terms of annihilation and creation operators expectation values by

$$\begin{aligned}\langle(\Delta\hat{x})^2\rangle = \frac{1}{4} + \frac{1}{4}\Bigg\{&\langle(\hat{b}_1^{\dagger 2} + \hat{b}_1^2 + \hat{b}_1^{\dagger 2}\hat{b}_1)\rangle \sin^2\left(\frac{\pi}{4} - \xi\right) \\ &+ \langle(\hat{b}_2^{\dagger 2} + \hat{b}_2^2 + \hat{b}_2^{\dagger 2}\hat{b}_2^2)\rangle \cos^2\left(\frac{\pi}{4} - \xi\right) \\ &+ \langle(\hat{b}_1\hat{b}_2 + \hat{b}_1\hat{b}_2^\dagger + \hat{b}_2\hat{b}_1^\dagger + \hat{b}_1^\dagger\hat{b}_2^\dagger)\rangle \cos 2\xi \\ &- \left[\langle(\hat{b}_1 + \hat{b}_1^\dagger)\rangle \sin\left(\frac{\pi}{4} - \xi\right) + \langle(\hat{b}_2 + \hat{b}_2^\dagger)\rangle \cos\left(\frac{\pi}{4} - \xi\right)\right]^2\Bigg\}.\end{aligned} \tag{27}$$

In our numerical computation for discussing the temporal behavior of $\langle(\Delta\hat{x})^2\rangle$, we have considered two different cases provided that $\theta = 0$, and $\phi = 0$. One when we take the value $\alpha_1 = -\alpha_2 = 3$ and plotted Fig. 3(a) and (b), and the second when we take $\alpha_1 = \alpha_2 = 3$, and plotted Fig. 3(c)–(f). For the first case we have taken the coupling parameters ratio $\lambda_1/\lambda_2 = 1.1$, and the system at exact resonance $\Delta = 0$. In this case we can see a small amount of squeezing, however when the detuning parameter takes place $\Delta = 4$ (off-resonance case) we observe an increase in the

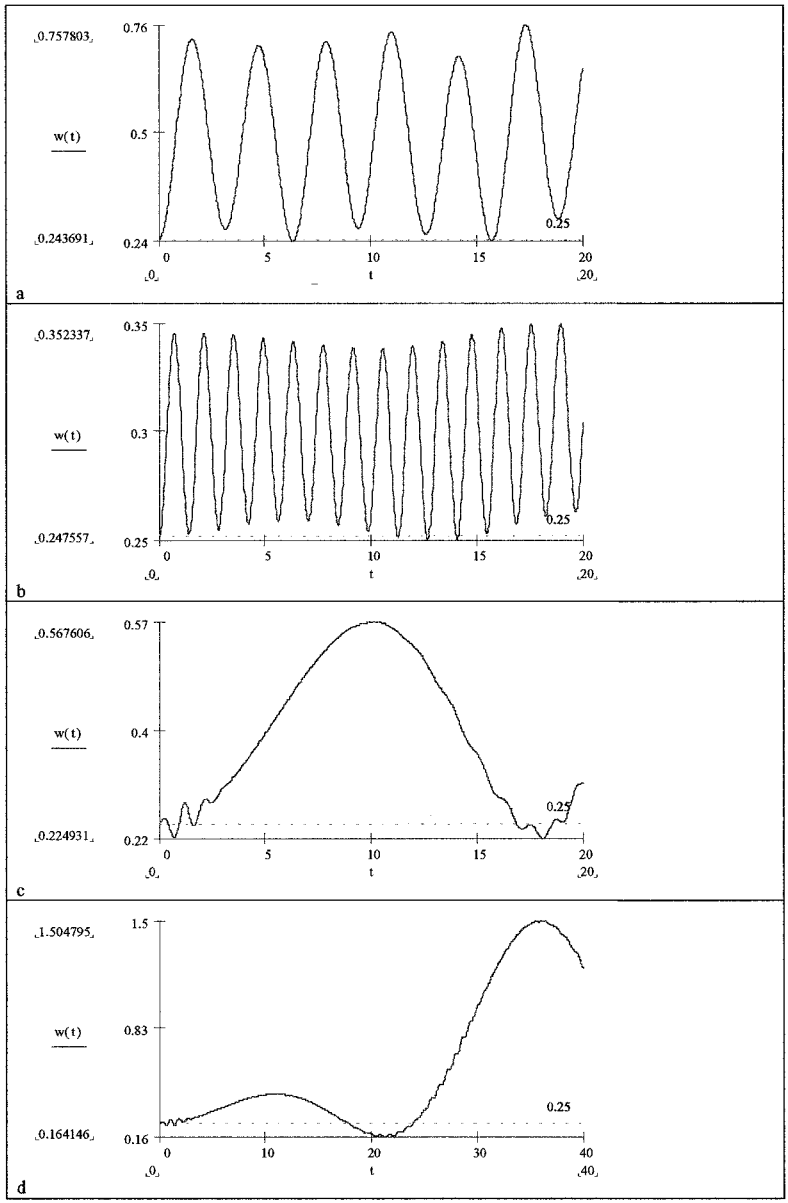

Fig. 3. Time evolution of the quantum fluctuations $(\Delta x)^2$ against time t the atom initially in excited state ($\theta = 0$ and $\phi = 0$) and the field is prepared in some different cases. (a) $\alpha_1 = -\alpha_2 = 3$, $\lambda_1/\lambda_2 = 1.1$ and $\Delta = 0$; (b) $\Delta = 4$ and other parameters same as (a); (c) $\alpha_1 = \alpha_2 = 3$, $\lambda_1/\lambda_2 = 0.1$ and $\Delta = 0$; (d) $\Delta = 4$ and other parameters same as (c); (e) $\alpha_1 = \alpha_2 = 3$, $\lambda_1/\lambda_2 = 1.1$ and $\Delta = 0$; (f) $\Delta = 4$ and other parameters same as (e).

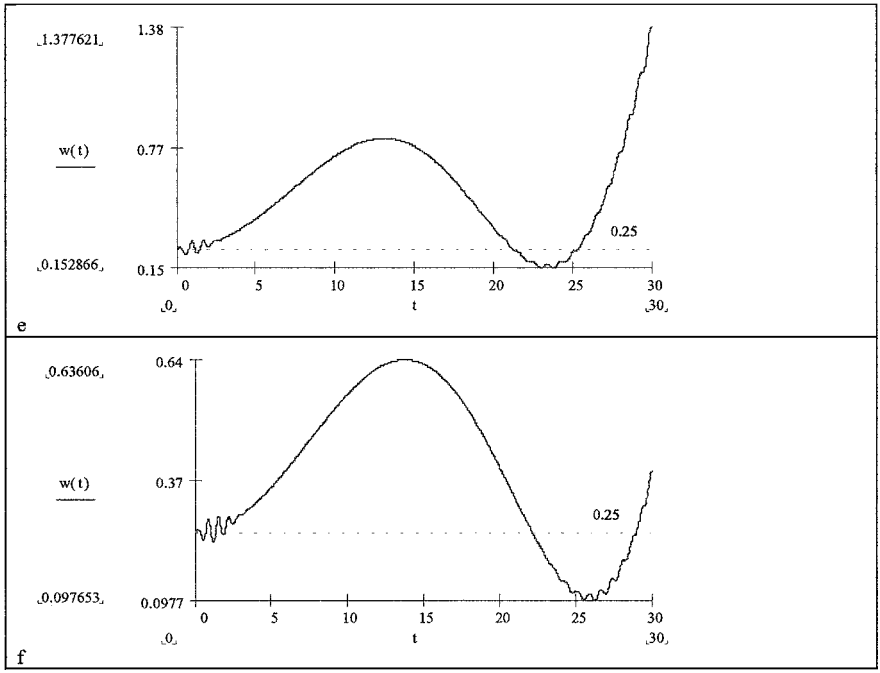

Fig. 3. (*Continued.*)

number of the fluctuations with an decrease in its maximum value. The squeezing amount in this case is too small and occurred for a short period of the time, see Fig. 3(a) and (b). For the other case where the field parameters $\alpha_1 = \alpha_2 = 3$ and the ratio of the coupling parameters $\lambda_1/\lambda_2 = 0.1$, we can observe the squeezing occurred just twice for both resonance $\Delta = 0$, and off-resonance $\Delta = 4$, cases within short period of the time, however the amount of the squeezing in the off-resonance case is much larger then the exact resonance case, see Fig. 3(c) and (d). This phenomenon gets more pronounced in the strong field case, for example when we increase the ratio of the coupling parameters $\lambda_1/\lambda_2 = 1.1$, where we can see the maximum value of the squeezing is also increased, see Fig. 3(e) and (f).

6. SECOND-ORDER CORRELATION FUNCTION

As another example of nonclassical of light we introduce in this context is the sub-Poissonian light which can be measured by photodetectors. A state (of a single mode for convenience) which displays sub-Poisson statistics is characterized by the fact that the variance of the photon number $\langle(\Delta\hat{n}_i(t))^2\rangle$ is less then the average photon number $\langle\hat{a}_i^\dagger(t)\hat{a}_i(t)\rangle = \langle\hat{n}_i(t)\rangle$. This can be expressed by means of the

normalized normal second-order correlation function as (Loundon, 1983).

$$g_i^{(2)}(t) = \frac{\langle \hat{a}_i^{\dagger 2}(t)\hat{a}_i^2(t)\rangle}{\langle \hat{a}_i^{\dagger}(t)\hat{a}_i^2(t)\rangle^2} = 1 + \frac{\langle (\Delta \hat{n}_i(t))^2\rangle - \langle \hat{a}_i^{\dagger}(t)\hat{a}_i(t)\rangle}{\langle \hat{a}_i^{\dagger}(t)\hat{a}_i(t)\rangle^2}, \tag{28}$$

where the subscript i relates to the ith mode. Then it holds that $g_i^{(2)}(t) \prec 1$ for sub-Poissonian distribution, $g_i^{(2)}(t) \succ 1$ for super-Poissonian distribution and when $g_i^{(2)}(t) = 1$ Poisson distribution of photons occurs. To discuss the behavior of the correlation function related to the present system we have to calculate the quantities $\langle \hat{a}_i^{\dagger 2}\hat{a}_i^2\rangle$, $i = 1, 2$ by means of the rotating transformation (4). In the first mode case we have the expression

$$\begin{aligned}\langle \hat{a}_1^{\dagger 2}\hat{a}_1^2\rangle &= \langle \hat{b}_1^{\dagger 2}\hat{b}_1^2\rangle \cos^4\xi + \langle \hat{b}_2^{\dagger 2}\hat{b}_2^2\rangle \cos^4\xi \\ &\quad + \frac{1}{2} Re\langle (\hat{b}_1^{\dagger 2}\hat{b}_2^2)\rangle \sin^2 2\xi + Re\langle (\hat{b}_1^{\dagger 2}\hat{b}_1\hat{b}_2)\rangle \cos^2\xi \sin^2 2\xi \\ &\quad - 2Re\big(\langle \hat{b}_1\hat{b}_2^{\dagger 2}\hat{b}_2\rangle\big) \cos^2\xi \sin 2\xi + \langle \hat{b}_1^{\dagger}\hat{b}_1\hat{b}_2^{\dagger}\hat{b}_2\rangle \sin^2 2\xi \end{aligned} \tag{29}$$

and

$$\begin{aligned}\langle \hat{n}_1(t)\rangle &= \langle \hat{a}_1^{\dagger}(t)\hat{a}_1(t)\rangle \\ &= H(1,1,0,0)\cos^2\xi + Re(H(1,0,0,1))\sin 2\xi \\ &\quad + H(0,0,1,1)\sin^2\xi \end{aligned} \tag{30}$$

Similarly for the second mode we have the following:

$$\begin{aligned}\langle \hat{a}_2^{\dagger 2}\hat{a}_2^2\rangle &= \langle \hat{b}_1^{\dagger 2}\hat{b}_1^2\rangle \sin^4\xi + \langle \hat{b}_2^{\dagger 2}\hat{b}_2^2\rangle \cos^4\xi \\ &\quad + \frac{1}{2} Re\big(\langle \hat{b}_1^{\dagger 2}\hat{b}_2^2\rangle\big) \sin^2 2\xi - Re\big(\langle \hat{b}_1^{\dagger 2}\hat{b}_1\hat{b}_2\rangle\big) \sin^2\xi \sin^2 2\xi \\ &\quad - 2Re\big(\langle \hat{b}_1\hat{b}_2^{\dagger 2}\hat{b}_2\rangle\big) \cos^2\xi \sin 2\xi + \langle \hat{b}_1^{\dagger}\hat{b}_1\hat{b}_2^{\dagger}\hat{b}_2\rangle \sin^2 2\xi \end{aligned} \tag{31}$$

and

$$\begin{aligned}\langle \hat{n}_2(t)\rangle &= \langle \hat{a}_2^{\dagger}(t)\hat{a}_2(t)\rangle \\ &= H(1,1,0,0)\cos^2\xi - Re(H(1,0,0,1))\sin 2\xi \\ &\quad + H(0,0,1,1)\sin^2\xi. \end{aligned} \tag{32}$$

Now let us discuss the numerical results for the function $g_1^{(2)}(t)$ when the field state initially in coherent state and the atom in the excited state. As before we shall consider the case in which field parameters $\alpha_1 = -\alpha_2 = 3$, and the coupling parameters ratio $\lambda_1/\lambda_2 = 1.1$. In absence of the detuning parameter $\Delta = 0$, (exact resonance case) we can see regular fluctuations behavior and the function is almost

super-Poissonian (thermal distribution), where the field shows Poisson distribution at some interval. When the detuning parameter takes place $\Delta = 4$, (off-resanonce case) we can see more fluctuations in the function behavior with observation of super and sub-Poissonian distribution. However the value of the themal distribution is much greater than the sub-Poissonian distribution, see Fig. 4(a) and (b). As soon as we take $\alpha_1 = \alpha_2 = 3$, while the value of the coupling parameters ratio $\lambda_1/\lambda_2 = 0.1$, a drastically changing occur in the function behavior. In this case when $\Delta = 0$ the function shows oscillation between super-Poissonian and sub-Poissonian distribution. The minimum value of the function occurs at the half time of the interaction period, showing sub-Poissonian behavior. This behavior is not quite in presence of the detuning parameter $\Delta = 4$, where we observe more decreasing in the minimum value followed by more increasing in the maximum value. However, this behavior takes time longer than that the exact resonance case, see Fig. 4(c) and (d). More increase in the coupling parameters ratio $\lambda_1/\lambda_2 = 1.1$, leads to more decrease in the sub-Poissonian interval, see Fig. 4(e) and (f). Finally we may point out that as a result of the similarity between Eqs. (28) and (31) then the behavior of the function $g_2^{(2)}(t)$ will be similar to that of $g_1^{(2)}(t)$.

7. Q-FUNCTION

In the following we shall concentrate on one of the most important quasi-probability distribution functions, thaat is the Q-function (Mollow and Glauber, 1967a,b). The Q-function is not only a convenient tool to calculate expectation values of antinormally ordered products of opeators, but also it gives us a new insight into the mechanism of the interaction for the model under consideration. It is well known that the Q-function can be defined in terms of diagonal elements of the density operator in the coherent state. Therefore we shall use the reduced density operator of the field $\rho^f(t)$ given by Eq. (20) to study the evolution of the quasi-probability distribution Q-function defined by

$$Q(\Gamma, t) = \frac{1}{\pi}\langle\Gamma|\rho^f(t)|\Gamma\rangle\frac{1}{\pi}\sum_{l,m=0}^{\infty}\rho_{l,m}^f(t)\frac{(\Gamma^*)^l(\Gamma)^m}{\sqrt{l!m!}}, \tag{33}$$

where $|\Gamma\rangle$ is a coherent state. Provided we define $\Gamma = x + iy$, then in Fig. (5) we have sketched the Q-function for the field initially in a coherent state and the atom in its excited state. As usual we fixed $\theta = 0$, and $\phi = 0$, where we considered the case in which the field parameters $\alpha_1 = -\alpha_2 = 3$, and the coupling parameters ratio $\lambda_1/\lambda_2 = 1.1$. i.e., the field is almost vacuum. Initially at time $t = 0$ we observe the function has only one peak centered at the origin (0,0), see Fig. 5(a), and as time develops it does not change its position. However, for the other cases of moderate or strong fields as the time develops the function splits into two peaks moving into opposite directions until they meet again at the revival time, see Fig. 5(f). That is,

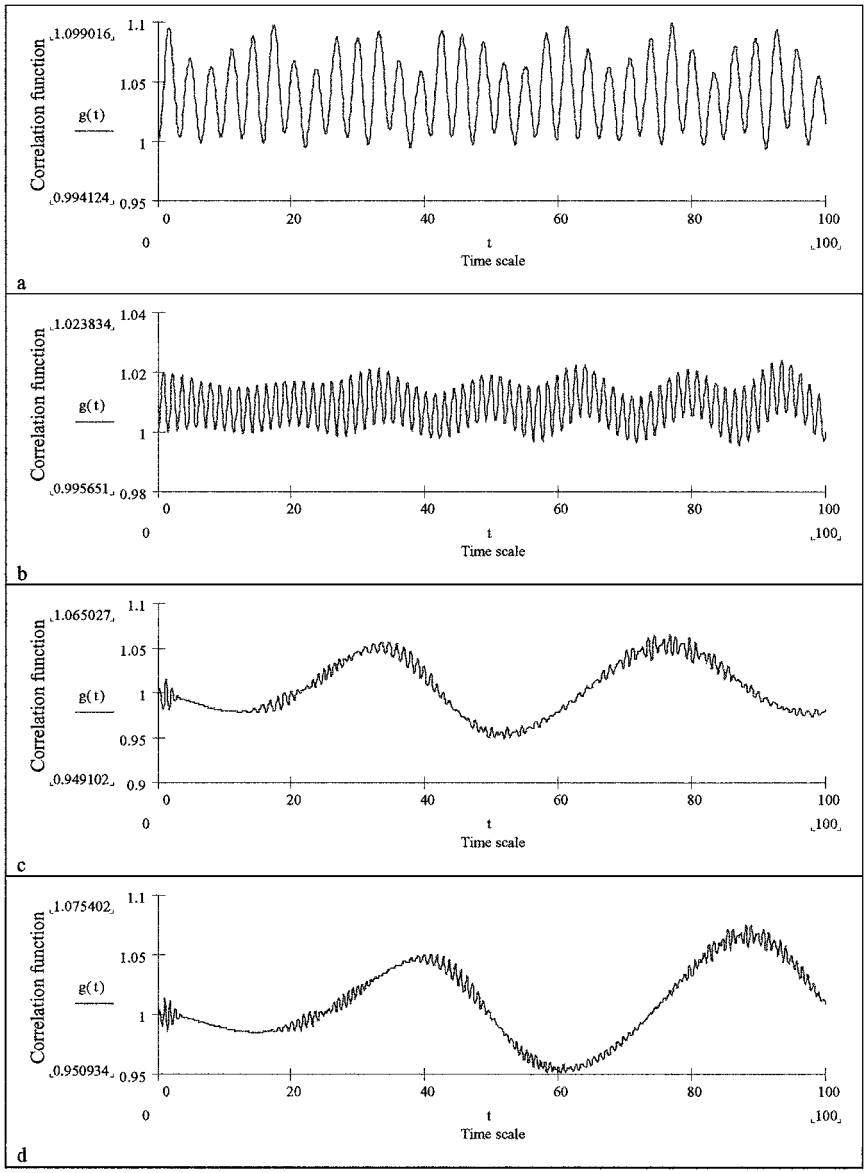

Fig. 4. Time evolution of the Correlation function $g_1^{(2)}(t)$ against time t the atom initially in excited state ($\theta = 0$ and $\phi = 0$) and the field is prepared in some different cases. (a) $\alpha_1 = -\alpha_2 = 3$, $\lambda_1/\lambda_2 = 1.1$ and $\Delta = 0$; (b) $\Delta = 4$ and other parameters same as (a); (c) $\alpha_1 = \alpha_2 = 3$, $\lambda_1/\lambda_2 = 0.1$ and $\Delta = 0$; (d) $\Delta = 4$ and other parameters same as (c); (e) $\alpha_1 = \alpha_2 = 3$, $\lambda_1/\lambda_2 = 1.1$ and $\Delta = 0$; (f) $\Delta = 4$ and other parameters same as (e).

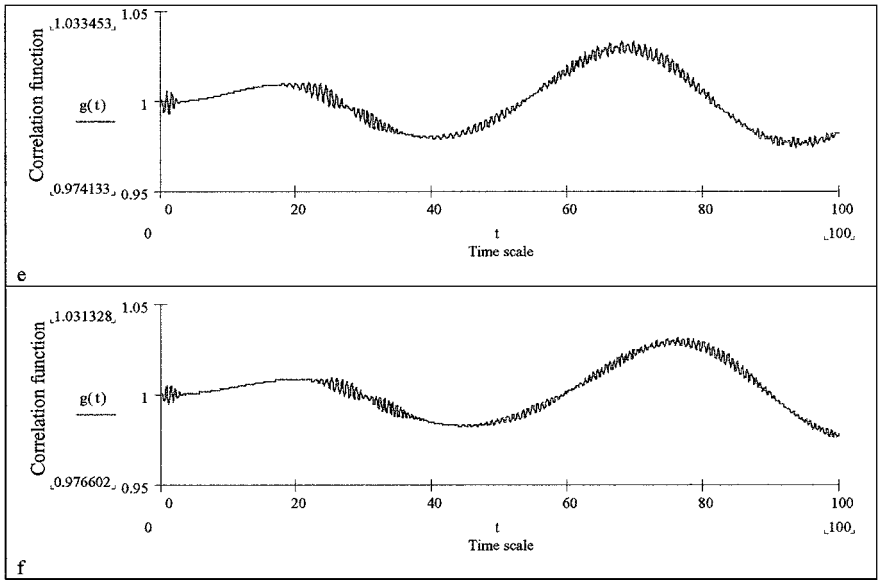

Fig. 4. (*Continued.*)

as time develops the two-peak move in the opposite directions around a circular path whose radius equals the square root of the initial mean photon number $\bar{n}_2$, and the peaks meet at the opposite side of the circle from the start at the revival time. The two peaks are symmertic at exact resonance, this is observed at half the revival time when we take $\Delta = 0$, and $\alpha_1 = \alpha_2 = 3$, while $\lambda_1/\lambda_2 = 1.1$ or 0.1, see Fig. 5(b) and (d). In the other case when we take the detuning parameter into account the function shows asymmetric stretching between the two peaks. Asymmetry behavior is observed for this case of detuning in Figs. 5(c) and (e). It is to be observed that increasing the mean photon number in the field results in spreading the Q-function in the phase space and hence an increase in the peak contour resultant of increasing the coupling parameter ratio.

8. PHASE DISTRIBUTION

Barnett and Pegg defined a Hermitian phase operator in a finite dimensional state space (Barnett and Pegg, 1989; Obada *et al.*, 1998, 1999; Pegg and Barnett, 1988, 1989, 1997). They used the fact that, in this state space one can define phase states rigorously. Thus the phase operator is defined as the projection operator on the particular phase state multiplied by the corresponding value of the phase. In fact the phase operator can be employed to investigate the phase properties of

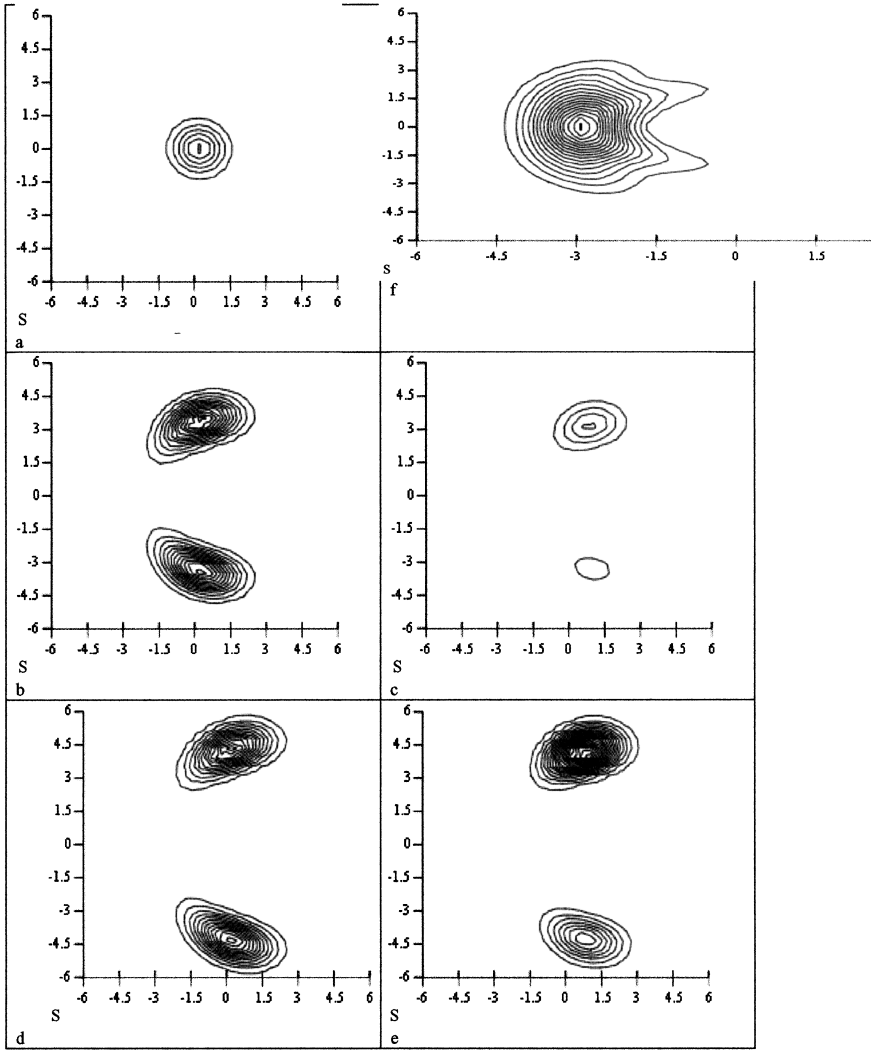

Fig. 5. The evolution of the Q-function against (x, y) the atom initially in excited state ($\theta = 0$ and $\phi = 0$) where $t = \frac{1}{2}t_r$ and the field is prepared in some different cases. (a) $\alpha_1 = -\alpha_2 = 3$, $\lambda_1/\lambda_2 = 1.1$ and $\Delta = 0$; (b) $\Delta = 4$ and other parameters same as (a); (c) $\alpha_1 = \alpha_2 = 3$, $\lambda_1/\lambda_2 = 0.1$ and $\Delta = 0$; (d) $\Delta = 4$ and other parameters same as (c); (e) $\alpha_1 = \alpha_2 = 3$, $\lambda_1/\lambda_2 = 1.1$ and $\Delta = 0$; (f) $\Delta = 4$ and other parameters same as (e).

quantum state for a single mode of the electromagnetic field. Furthermore, it can be easily extended to include the two-mode field which is also of interest in the field of quantum optics. In the following we shall study the phase properties of the present system in a light of the Pegg–Barnett phase formalism. If we consider the field initially prepared in a coherent state then the Pegg–Barnett phase distribution $P(\zeta, t)$ can be written as an infinite sum, thus

$$P(\zeta, t) = \frac{1}{2\pi} \sum_{l,m=0}^{\infty} \rho_{l,m}^{f}(t) \exp[i(l-m)(\zeta - \zeta_0)], \tag{34}$$

where ζ_0 is the phase reference angle and $\rho_{l,m}^{f}(t)$ is the density matrix operator. Alternatively we may take ζ_0 to be zero and rewrite the phase distribution in the form

$$P(\zeta, t) = \frac{1}{2\pi} \left\{ 1 + 2Re \sum_{l,j=0;j\geq l}^{\infty} \rho_{l,j}^{f}(t) \exp[i(j-l)\zeta] \right\}, \tag{35}$$

We have computed the phase probability distribution function, related to a more generalized system of a two-level atom in interaction with a two-mode but after some specific transformation converted to one-mode as shown above. In our computations, the field is initially in coherent states and the atom in excited state. In Fig. 6 the phase distribution $P(\zeta, t)$ is plotted against ζ and time t.

For the case of the almost vacuum (see the parameters taken above in the previous sections) we see that the distribution is almost flat with a hump around $\zeta = 0$ and this figure changes slightly as time develops see Fig. 6(a). The case changes slightly as the case of off-resonance is taken into consideration as can be seen from Fig. 6(b). This can be related to the phase space plot of the Q-function shown in Fig. 5(a) where it is centered unmoved at the origin. While for the case of moderate and strong fields and at $t = 0$ only one peak in the middle appears at $\zeta = 0$, the peak is symmetric about $\zeta = 0$. As time t increases the peak in the middle splits into two peaks diverging away from the middle towards the wings $\zeta = \pm\pi$ where they meet them at $t = t_{\mathrm{R}}$ but as the time increses the two wings converge towards the middle $\zeta = 0$ at $t = 2t_{\mathrm{R}}$. In the case of resonance the figure is symmetric around $\zeta = 0$ as can be seen from Figs. 5(c) and (e) where the two-peak figure shows this symmetry. On the other hand this symmetry is broken in the case of off-resonance where one of the peaks is subdued while the second peak is raised. The reason is due to the amplitudes of the two rotating peaks where one of them has higher value than the other as depicted in the figures for the Q-function (Obada *et al*. 1998 and 1999).

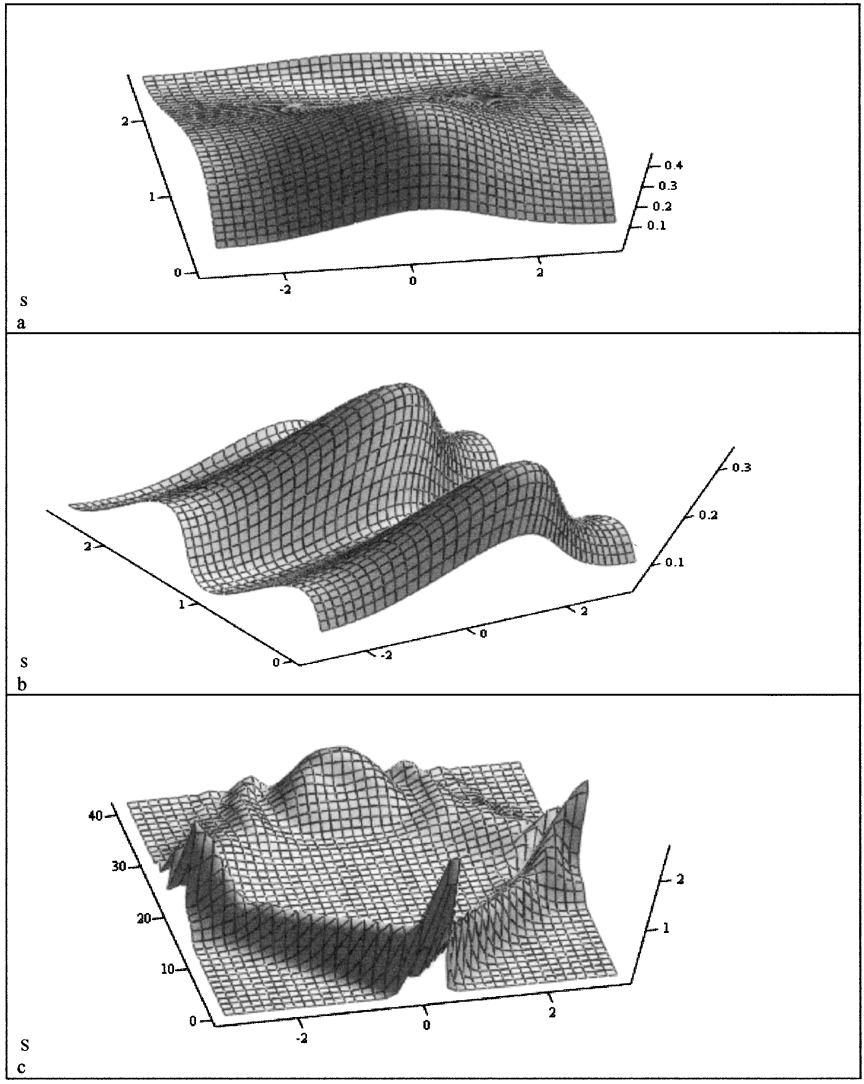

Fig. 6. The evolution of the phase distribution against (η, t) the atom initially in excited state ($\theta = 0$ and $\phi = 0$) and the field is prepared in some different cases. (a) $\alpha_1 = -\alpha_2 = 3$, $\lambda_1/\lambda_2 = 1.1$ and $\Delta = 0$; (b) $\Delta = 4$ and other parameters same as (a); (c) $\alpha_1 = \alpha_2 = 3$, $\lambda_1/\lambda_2 = 0.1$ and $\Delta = 0$; (d) $\Delta = 4$ and other parameters same as (c); (e) $\alpha_1 = \alpha_2 = 3$, $\lambda_1/\lambda_2 = 1.1$ and $\Delta = 0$; (f) $\Delta = 4$ and other parameters same as (e).

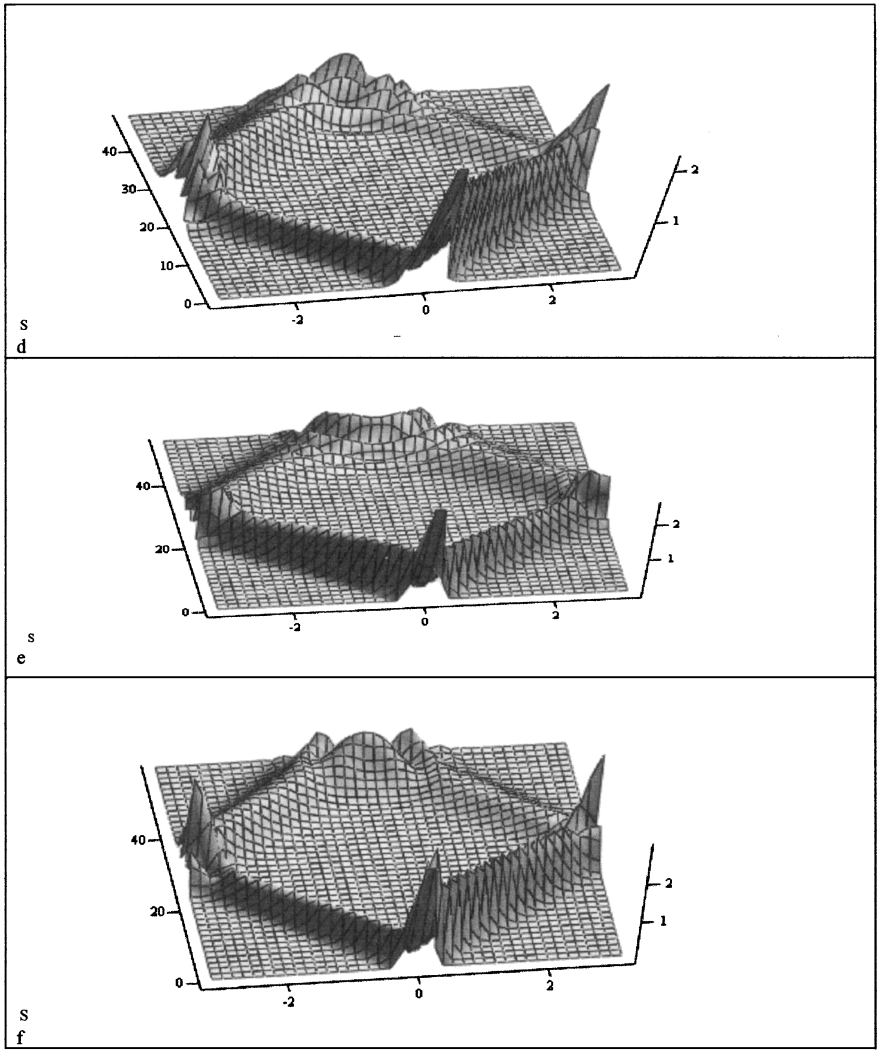

Fig. 6. (*Continued.*)

9. QUANTUM FIELD ENTROPY

Since the field entropy can be used as a measurement of the degradation of entanglement between the field and the atom, we devote the present section to discuss the degree of entanglement for the present system. The quantum dynamics described by the Hamiltonian (3) leads to an entanglement between the field and

the atom, which will be quantified by the field entropy. From quantum mechanics point of view the von Neumann entropy of the state p (the density operator for a given quantum system) is defined as

$$S = \mathrm{Tr}\{\rho \ln \rho\}, \tag{36}$$

where we have set Boltzmann's constant $\kappa = 1$. If ρ describes a pure state, the $S = 0$, and if ρ describes a mixed state, then $S \neq 0$. Araki and Lieb showed that these entropies satisfy the triangle inequalities $|S_a - S_f| \leq S \leq S_a + S_f$. Quantum entropies are generally difficult to compute because they involve the diagonalization of large (and, in many cases, infinite dimensional) density matrices. Thus explicit illustrations of the inequalities $|S_a - S_f| \leq S \leq S_a + S_f$ are difficult. The authors of references (Phoenix and Knight, 1988, 1991a,b) succeeded to evaluate the field entropy in a closed form and showed that it did indeed equal the atomic entropy at all times in the context of the Jaynes–Cummings model. They considered a two-level atom interacting with an undamped cavity initially in a coherent state. In this case the composite entropy is initially zero and remains zero at all times since the atom-field system is isolated from its environment. If the system is closed, then we have $S_f = S_a$, for the entropy of a general two-component system. One immediate consequence of this inequality is that if the total system is prepared in a pure state then the component systems have equal entropies. Since our Hamiltonian model can be regarded as a generalization of JCM, we shall follow the method adopted earlier to calculate the atomic entropy. The entropies of the atom and the field, when treated as a separate system, are defined through the corresponding reduced density operators by

$$S_{a(f)} = \mathrm{Tr}_{a(f)}\{\rho_{a(f)} \ln \rho_{a(f)}\} \tag{37}$$

provided we treat both separately. Since the trace is invariant under a similarity transformation, then we can go to a basis in which the density matrix of the field is diagonal and then express the field entropy $S_f(t)$ in terms of the eigenvalue $\lambda_f^{\pm}(t)$, for the reduced field density operator. To calculate the various field eigenstates in a simple way, a general method has been developed by Phoenix and Knight (1988, 1991a,b). By applying this method, we can obtain the eigenvalues for the reduced density operator thus,

$$\begin{aligned} \lambda_f^{\pm}(t) &= \langle A(t)|A(t)\rangle \pm \exp[\mp\varsigma]|\langle A(t)|B(t)\rangle| \\ &= \langle B(t)|B(t)\rangle \pm \exp[\mp\varsigma]|\langle B(t)|A(t)\rangle|, \end{aligned} \tag{38}$$

where

$$\varsigma = \sin \mathrm{h}^{-1}\left(\frac{\langle A(t)|A(t)\rangle - \langle B(t)|B(t)\rangle}{2|\langle A(t)|B(t)\rangle|}\right). \tag{39}$$

Thus the field entropy $S_f(t)$ may be expressed in terms of the eigenvalues $\lambda_f^{\pm}(t)$ for the reduced field density operator as,

$$S_f(t) = -[\lambda_f^+(t)\ \ln \lambda_f^+(t) + \lambda_f^-(t)\ \ln \lambda_f^-(t)]. \tag{40}$$

In the following we shall use Eq. (40) to discuss the degree of entanglement for the present model. For this reason we have considered in our numerical computations the parameters θ and ϕ are zero. Thus for different values of both the mean photon numbers α_i, $i = 1, 2$ and the coupling parameters ratio λ_1/λ_2, we plotted Fig. (7). For example when we set $\alpha_1 = -\alpha_2 = 3$, and $\lambda_1/\lambda_2 = 1.1$ and in absence of the detuning parameter (resonances case), we observe a rapid fluctuations during the course of interaction. This can be seen in Fig. 7(a) where the entropy function varies between its maximum and its minimum value. This means that there is a fast collapses and revivals during the interaction period which leads to a strong and weak entanglement between the atom and the field. Moreover we can also see disentanglement at certain period of the time. On the other hand when the detuning parameter takes place $\Delta = 4$, (off-resonances case) we observe some changes occur in the function behavior. For example, we realize the entropy function reduced its maximum value. In the meantime the numbers of disentanglement period are also decreased. This decrement in the entropy function is nearly equivalent to half of the exact resonance case, see Fig. 7(b). Now let us turn our attention to consider the case in which the field parameters $\alpha_1 = \alpha_2 = 3$, and the ratio between the coupling parameters $\lambda_1/\lambda_2 = 0.1$. In this case the behavior of the entropy function is drastically changed. For instance, there is no disentanglement can be observe at any period of the time during the course of interaction. Further the greatest decrement in the field entropy occurs after a short period of time, followed by an increase in the value of the entropy. As the time developes we realize there is an increase in the entropy value in addition to irregular fluctuations behavior; see Fig. 7(c). Weak entanglement can be observed in presence of the detuning parameter where the maximum value of the entropy in this case is decreased, in the meantime the function shows an increase in it minimum value, see Fig. 7(d). Comparing with the previous case, any change in the value of the coupling parameters ratio $\lambda_1/\lambda_2 = 1.1$ leads to increase in the entropy maximum value after onset of the interaction provided $\Delta = 0$. However we can also see a decrease in the minimum value just for short period of the time. This is followed by irregular fluctuations with more increasing in function value, see Fig. 7(e). When we take $\Delta = 4$ similarly behavior to that of the previous cases can be seen but with more revival in the function, provided the coupling parameters ratio unchanged, see Fig. 7(f). Finally, we may conclude that in absence of the detuning parameter (exact resonance case) the entropy function reaches both absolute maximum and absolute minimum of its value. However, existence of the detuning parameter (off-resonance case) decreases the maximum value and increases the minimum value

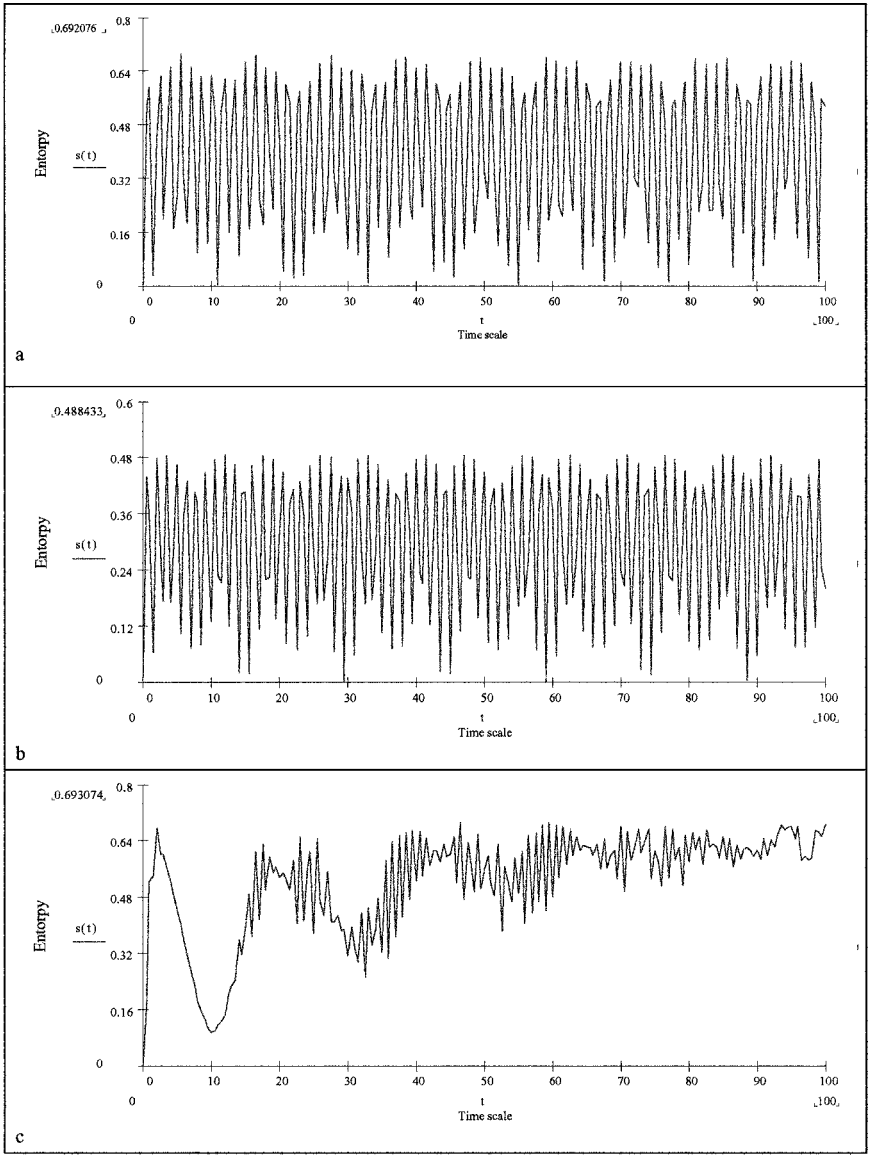

Fig. 7. (a) The evolution of the field entropy against t the atom initially in excited state ($\theta = 0$ and $\phi = 0$) and the field is prepared in some different cases. (a) $\alpha_1 = -\alpha_2 = 3$, $\lambda_1/\lambda_2 = 1.1$ and $\Delta = 0$; (b) $\Delta = 4$ and other parameters same as (a); (c) $\alpha_1 = \alpha_2 = 3$, $\lambda_1/\lambda_2 = 0.1$ and $\Delta = 0$; (d) $\Delta = 4$ and other parameters same as (c); (e) $\alpha_1 = \alpha_2 = 3$, $\lambda_1/\lambda_2 = 1.1$ and $\Delta = 0$; (f) $\Delta = 4$ and other parameters same as (e).

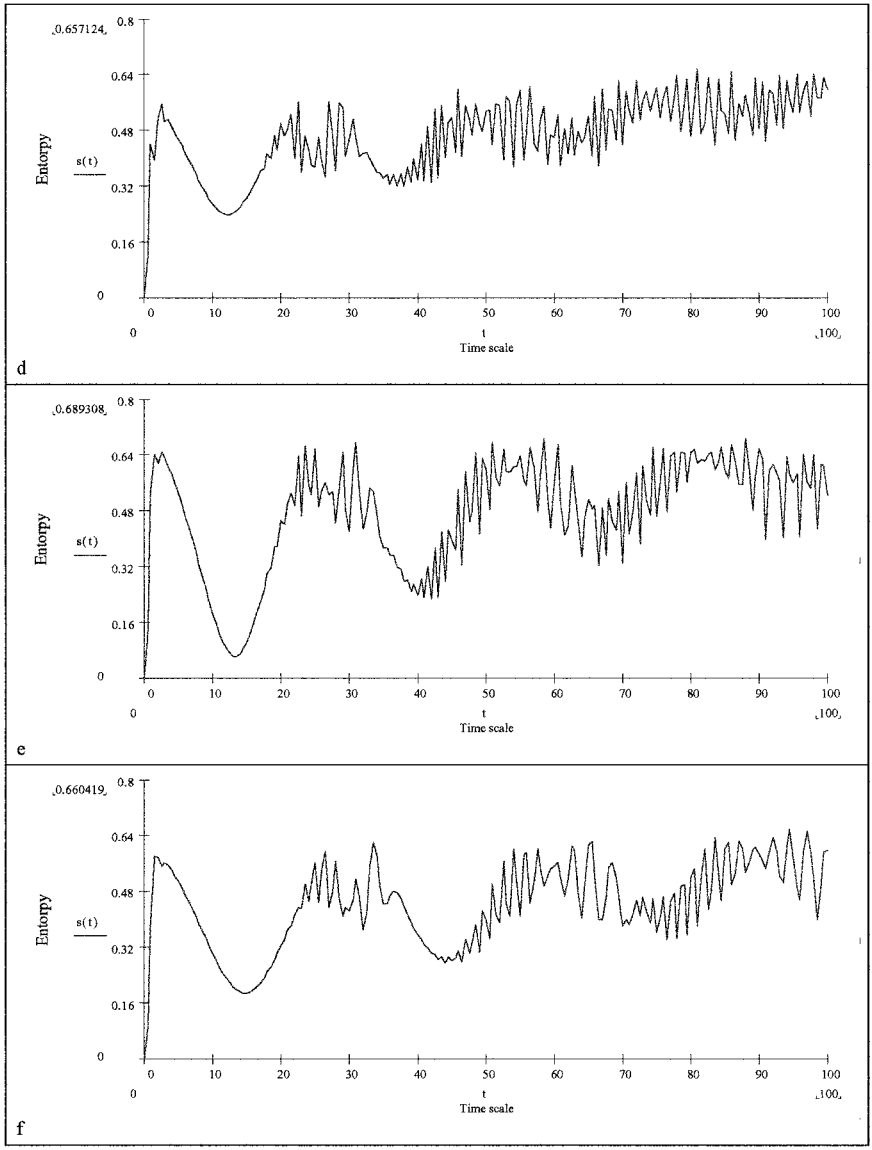

Fig. 7. (*Continued.*)

of the field entropy, and consequently we can obtain a variation in the degree of the entanglement. This phenomenon is in fact dominant in all the cases we have considered.

10. CONCLUSION

In the previous sections of the present paper we have considered the statistical properties of a new Hamiltonian model. This Hamiltonian represents the interaction between a single two-level atom and two fields injected simultaneously within a perfect cavity. The model can be regarded as a generalization of the Jaynes–Cummings model, or it can be regarded as a generalization of the parametric frequency converter model. Under a certain integrability condition we have obtained both the dynamical operators in the Heisenberg picture and the wavefunction in the Schrödinger picture, see Eq. (16). In obtaining the wavefunction representation we have taken the system to be initially in a correlated coherent state. This in fact gave us an advantage to see the interference between the two fields. Several statistical properties of the system have been discussed, for example atomic inversion, photon number distribution, and the squeezing phenomenon. Most of our discussion concentrated on the effect of the variation of the coupling parameters ratio, and the detuning parameter as well as the fields mean photon numbers. We have shown that in all cases the system is sensitive to any variation in these parameters. For example the degree of the entanglement is affected strongly when the fields mean photon numbers are changed.

REFERENCES

Abdalla, M. S., Ahmed, M. M., and Obada, A.-S. F. (1990). *Physica A* **162**, 215.
Abdalla, M. S., Ahmed, M. M., and Obada, A.-S. F. (1991). *Physica A* **170**, 393.
Abdalla, M. S., Abdel-Aty, M., and Obada, A.-S. F. (2002). *Optics Communications* **211**, 225.
Abdel-Aty, M., Abdalla, M. S., and Obada, A.-S. F. (2002). *Journal of Optics B: Quantum Semiclass Opticals* **4**, 134.
Abdalla, M. S., El-Orany, F. A. A., and Perina, J. (2001a). *European Physical Journal D* **13**, 423.
Abdalla, M. S., El-Orany, F. A. A., and Perina, J. (2001b). *IL-Nuovo Cimento B* **116**, 137.
Barnett, S. M. and Pegg, D. T. (1989). *Journal of Modern Optics* **36**, 7.
Bužek, V. and Jex, I. (1990). *Optics Communications* **78**, 425.
Bogolubov Jr, N. N., Le Kien, F., and Shumovski, A. S. (1984). *Physics Letters A*, **101**, 201.
Caves, C. M. and Schumaker, B. L. (1985). *Physical Reviews A* **31**, 3068.
Deng, Z. (1983). *Optics Communications* **54**, 222.
Diedrich, F. and Walther, H. (1987). *Physical Review Letters* **58**, 203.
Eberly, J. H., Narozhny, N. B., and Sanchez-Mondragan, J. J. (1980) *Physical Review Letters* **44**, 1323.
El-Orany, F. A. A., Perina, J., and Abdalla, M. S. (2001a). *Physica Scripta A* **63**, 128.
El-Orany, F. A. A., Perina, J., and Abdalla, M. S. (2001). *Journal of Optics B: Quantum Semiclass Optics* **3**, 66.
El-Orany, F. A. A., Perina, J., and Abdalla, M. S. (2001). *International Journal of Modern Physics B* **15**, 2125.
Filipowicz, P., Javanainen, J., and Meystre, P. (1986). *Physical Review A* **34**, 3077.

Filipowicz, P., Meystre, P., Rempe, G., and Walther , H. (1985). *Optica Acta* **32**, 1105.
Gea-Banacloche, J. (1990). *Physical Review Letters* **65**, 3385.
Gea-Banacloche, J. (1991). *Physical Review A* **44**, 5913.
Gerry, C. C. and Hach III, E. E. (1993). *Physics Letter A* **179**, 1 .
Glauber, R. J. (1963). *Physical Review* **131**, 2766.
Gou, S.-C., Steinbach, J., and Knight, P. L. (1997). *Physical Review A* **55**, 3719.
Guzman, A. M., Meystre, P., and Wright, E. M. (1989). *Physical Review A* **40**, 2471.
Jaynes, E. T. and Cummings, F. W. (1963). *Proceedings of the IEEE* **51**, 89.
Joshi, A. and Lawande, S. V. (1991). *Journal of Modern Optics* **38**, 1407.
Joshi, A. and Puri, R. R. (1992). *Physical Review A,* **45**, 5056.
Knight, P. L. and Radmore, P. M. (1982). *Physics Letters A* **90**, 342.
Kuklinski, J. R. and Madajczyk, J. L. (1988). *Physical Review A* **37**, 3175.
Loundon, R. (1983). *The Quantum Theory of Light*, Clarendon Press, Oxford.
Loundon, R. and Knight, P. L. (1987). *Squeezed Light, Journal of Modern Optics*, **34** (Special issue).
Makhviladze, T. M. and Shelepin, L. A. (1974). *Physical Review A*, **9**, 538.
Meschede, D., Walther, H., and Muller, G. (1985). *Physical Review Letters* **54**, 551.
Meystre, P. and Walls, D. F. (eds.) (1991). *Selected Papers on Nonclassical Effect in Quantum Optics*, (AIP, New York).
Meystre, P. and Zubairy, M. S. (1982). *Physics Letter A* **89**, 390.
Milonni, P. W., Ackerhalt, J. R., and Galbraith, H. W. (1983a). *Physical Review Letters* **50**, 966.
Milonni, P. W., Ackerhalt, J. R., and Galbraith, H. W. (1983b). *Physical Review Letters* **51**, 1108.
Mollow, B. R. and Glauber, R. J. (1967a). *Physical Review* **160**, 1076.
Mollow, B. R. and Glauber, R. J. (1967b). *Physical Review* **160**, 1097.
Moya-Cessa, H., Bužek, V., and Knight, P. L. (1991). *Optics Communications* **85**, 267.
Moya-Cessa, H. and Vidiella-Barranco, A. (1995). *Journal of Modern Optics* **42**, 1547.
Narozhny, N. B., Sanchez-Mondragan, J. J., and Eberly, J. A. (1981). *Physical Review A* **23**, 2361.
Obada, A.-S. F., Abdel-Hafez, A. M., and Abdel-Aty, M. (1998). *European Physics Journal D* **3**, 289.
Obada, A.-S. F., Abdel-Hafez, A. M., and Abdel-Aty, M. (1999). *Physica Scripta* **60**, 329.
Pegg, D. T. and Barnett, S. M. (1997). *Quantum Optics* **2**, 225.
Pegg, D. T. and Barnett, S. M. (1988). *European Physical Letters* **6**, 483.
Pegg, D. T. and Barnett, S. M. (1989). *Physical Review A* **39**, 1665.
Phoenix, S. J. D. and Knight, P. L. (1991a). *Physical Review A* **44**, 6023.
Phoenix, S. J. D. and Knight, P. L. (1991b). *Physical Review Letters* **66**, 2833.
Phoenix, S. J. D. and Knight, P. L. (1988). *Annals of Physics (New York)* **186**, 381.
Puri, R. R. and Joshi, A. (1989). *Optics Communications* **69**, 369.
Rempe, G., Walther, H., and Klein, N. (1987). *Physical Review Letters* **58**, 353.
Schumaker, B. L. and Caves, C. M. (1985). *Physical Review A* **31**, 3093.
Shapiro, J. H. (1980). *Optics Letters* **5**, 351.
Shapiro, J. H., Yuen, H. P., and Machado, M. J. A. (1979). *IEEE Transaction on Information Theory* **IT25**, 179.
Shore, B. W. and Knight, P. L. (1993). *Journal of Modern Optics* **40**, 1195.
Short, R. G. and Mandel, L. (1983). *Physical Review Letters* **51**, 384.
Slosser, J. J. and Meystre, P. (1990). *Physical Review A* **41**, 3867.
Slosser, J. J., Meystre, P., and Braunstein, S. L. (1989). *Physical Review Letters* **63**, 934.
Tavis, M. and Cummings, F. W. (1966). *Physical Review* **170**, 379.
Vidiella-Barranco, A., Moya-Cessa, H., and Buzek, V. (1992). *Journal of Modern Optics* **39**, 1441.
Werner, M. J. and Risken, H. (1991a). *Quantum Optics* **3**, 185.
Werner, M. J. and Risken, H. (1991b). *Physical Review A,* **44**, 4623.
Yuen, H. P. and Shapiro, J. H. (1978). *IEEE Transaction on Information Theory* **IT24**, 657.
Yuen, H. P. and Shapiro, J. H. (1980). *IEEE Transaction on Information Theory* **IT26**, 78.